ROS and αSYN dynamics in Parkinson's Disease

Sara Baldinelli[1], Letizia De Pietri[1], Roan Spadazzi[1]

[1] *University of Trento, Trento 38123, Italy*

Introduction

Parkinson's Disease (PD) is the second most common neurodegenerative disease in the human brain, having a heterogeneous symptomatology, progression and risk factors [1]. Although the cause of PD is not completely known, it is now clear that an interplay of genetic and environmental factors is at the basis of this condition. Moreover, given its complexity, PD comes along with clinical challenges making the diagnosis and treatment of the symptoms particularly demanding [2].
Mathematical models constitute a robust framework to build and simulate representations of different phenomena. In this case, the creation of a model of PD allows the analysis and simulation of relevant pathways, pathogenesis, behavior over time and more, avoiding direct experimentation but rather replicating the events "in-silico". The modeled biological phenomena include a series of pathological processes, the most distinctive one being the high levels of Reactive Oxygen Species (ROS), leading to high oxidative stress that can be damaging for neurons. Together with ROS generation, another recurrent feature is the accumulation of misfolded α-synuclein (αSYN) protein. αSYN, associated with other proteins, can result in the formation of abnormal aggregations called Lewy Bodies (LB), known to be toxic and linked to cellular stress. Other characteristics have been linked to this disease, for example the disruption within mitochondria has implications in the regulation of calcium homeostasis. The interaction between ROS and αSYN is one of the main drivers in the neurodegenerative process. Excessive ROS levels induce oxidative modifications of αSYN, promoting its aggregation. In turn, αSYN aggregates impair mitochondrial function, increasing ROS production and creating a self-reinforcing cycle. This leads to oxidative stress, neuroinflammation, synaptic dysfunction, and neuronal death. Targeting ROS levels and αSYN clearance is a key therapeutic strategy to disrupt this harmful cycle.

1. Model Description

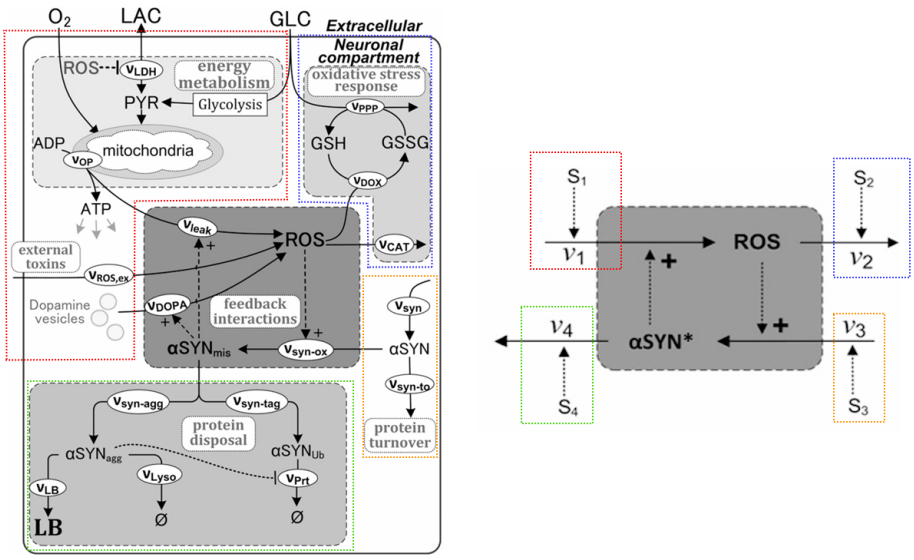

Figure 1. Side-by-side schematization of the two models (Comprehensive and Simple); the colored squares represent the simplification steps to switch from the complete to the simple model. red: internal and external oxidative stresses and toxins; blue: anti-oxidative mechanisms; yellow: genetic mechanisms and αSYN expression; green: protein clearance mechanisms and LB.

1.1 Comprehensive PD model

The 4 macro-pathways taken into account to model PD [3] are energy metabolism, oxidative/anti-oxidative metabolism, αSYN metabolism and related damage, and protein disposal pathways together with LB accumulation. This model aims to represent the main reactions in generic neurons, without focusing on a specific neuronal subtype. Furthermore, since most molecules are present in large amounts, the system can be modeled by ordinary differential equations (ODEs). The model is calibrated using experimental data, replicating physiological behaviors while capturing pathological changes.

1.1.1 Energy Metabolism and Oxidative Stress

Energy metabolism models mitochondrial oxidative phosphorylation (*vOP*), involving ROS and ATP. Mitochondrial leak producing ROS (*vleak*) increases under pathological conditions due to interactions with misfolded αSYN. The model also integrates anti-oxidative pathways (*vPPP*, *vDOX*) and external ROS sources (*vROS,ex*), simulating the dynamics between the former and the latter.

1.1.2 αSYN Dynamics, Protein Turnover and Disposal

The metabolism of αSYN, starting from its genetic expression (*vsyn*), considers both its normal turnover pathway (*vsyn-to*) and its misfolding under oxidative stress (*vsyn-ox*). Misfolded αSYN clusters into insoluble aggregates (*αSYNagg*) that can further become LB (*vLB*) or can be removed from the system by the lysosomal action (*vLyso*). Also, misfolded αSYN is normally cleaved by the proteosome disposal pathway after being tagged by the Parkin protein (*vsyn-tag*).
Finally, note that a Hill kinetic is used to describe the non-linear interactions between misfolded αSYN and ROS release, highlighted in the "feedback interactions" box in **Fig. 1**.

1.1.3 Simulation Results and Analysis

This model was used to simulate PD dynamics under different risk factors: exposure to toxins, aging and genetic factors. Toxin exposure was simulated by applying external oxidative stress (continuously at low level or high short pulses). In the first simulation configuration no LB accumulation was observed, while in the second one it accumulates damaged αSYN moving to a new state with high ROS concentration, corresponding to the "disease state".
Aging is reproduced by decreasing mitochondrial efficiency over a period of 10 years (increasing leakage from 0.5% to 1.5% and from 0.5% to 3%). In the first simulation the system is able to maintain acceptable levels of ROS and αSYN, while in the second one the opposite happens and a disease state is reached.
The most well-known genes associated with PD are the *αSYN* gene and the *Parkin* gene. The over-expression of the *αSYN* gene is simulated by increasing the rate of its protein expression, while the mutations in the *Parkin* gene are reproduced by reducing the rate constant for the αSYN tagging reaction. To trigger the disease state, a 200% over-expression of *αSYN* or a 75% reduction in *Parkin*-induced tagging rate is needed.
Since PD is a multi-factorial condition, different tolerable factors were also combined together, for example moderate genetic predisposition and age risk. Although they are non-damaging when considered separately, their combination cannot be tolerated by the system.

1.2 Simplified PD model

Starting from the comprehensive model, a simplified one was created [4] by lumping into 4 reactions the processes associated to the central main "feedback motif" (highlighted in dark gray in **Fig. 1**). Internal/external oxidative stresses and mitochondrial activity are represented by the S_1 parameter. Anti-oxidative mechanisms and energy metabolism by S_2, genetic factors by S_3, and lastly protein disposal/clearance by S_4 with corresponding rates *v1*, *v2*, *v3* and *v4*. This simplification works because of the core behavior of the model (the central feedback loop that involves ROS and αSYN) that can capture the pathogenic features also seen in the comprehensive one. Simulating the other reactions as well would lead to having more variability, but with a qualitatively similar response. **Fig. 2a** shows that the simplified model emulates the dynamic behavior observed in the comprehensive one.

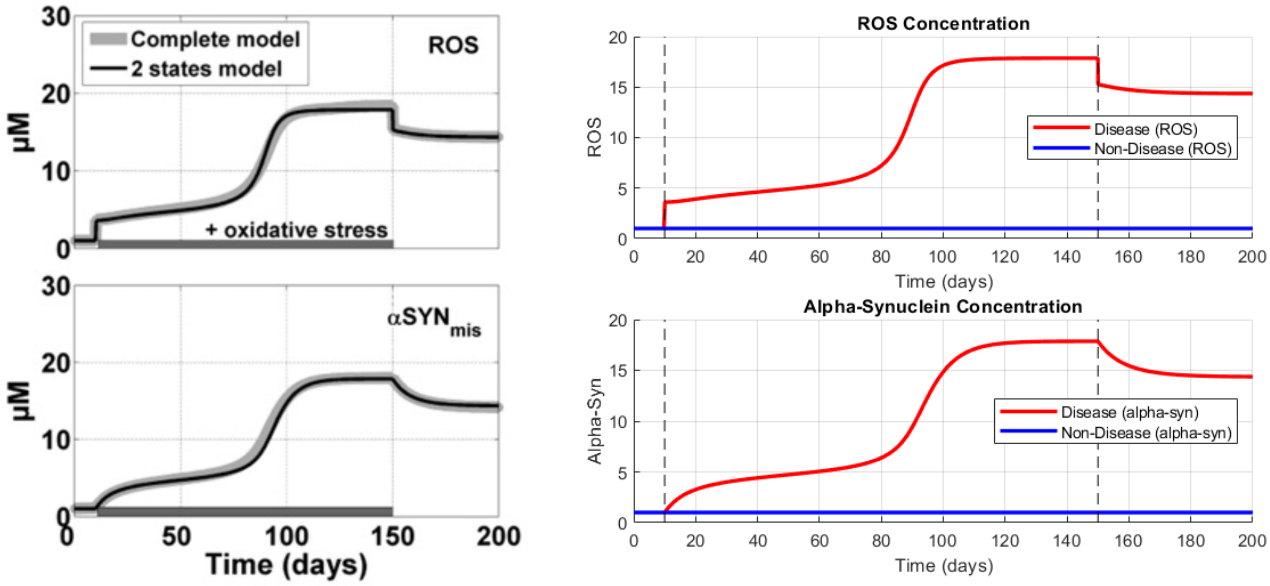

(a) Figure taken from the original paper.

(b) Figure made with our script.

Figure 2. Comparison between the original paper's image and ours; here an S_1 value of 2.6 is applied from days 10 to 150. The boundaries are highlighted by gray dashed lines. The red curve represents the "disease-state" conditions, the blue curve was obtained with the standard $S_{1,2,3,4}$ values of the "normal-state": 0, 1, 1, 1

2. Model Implementation

The simplified model was implemented in a Matlab script retrieved from the BioModels Database [5] and adapted to our needs. The implemented variables are the ROS and αSYN concentrations whose initial conditions are set to 1μM. Note that the system of ODEs is solved by calling the *ode23tb* function, tendentially suited for stiff trends and crude error tolerances. The script models both disease and non-disease conditions through the boolean *disease mode* variable. The main function *xdot* that computes the differential equations starts up the initial parameters (*compartment_Neuron*: volume scaling factor, k_1: ROS generation, k_2: ROS removal, k_3: αSYNmis generation, k_4: αSYNmis removal, $d_{\alpha SYN}$: increase in ROS release due to αSYN damage, $K_{\alpha SYN}$: Hill kinetic constant for αSYN damage; furthermore, the generalized objects S_1: internal/external oxidative stresses , S_2: age-related anti-oxidative mechanisms, S_3: influence of genetic damage/mutation, S_4: protein clearance mechanisms). The non-disease default parameters for S_1, S_2, S_3 and S_4 are respectively 0 (meaning no oxidative stress; a higher value leads to the disease-state), 1 (meaning full functioning of the anti-oxidative age related mechanisms; a lower value leads to the disease-state), 1 (corresponding to no relevant genetic predisposition; a higher value leads to the disease-state) and 1 (meaning full functioning of the protein clearance mechanisms; a lower value leads to the disease-state). Then, the four reactions (also visible in **Fig. 1**) are modeled, each with its own function (V1, V2, V3, V4) using *compartment_Neuron* as a scaling factor. Lastly, the *piecewise* function is useful to modify a parameter of the model for a specific amount of time. It is helpful to notice that the concentrations are measured in μM and time in days, as it has to consider both ROS and αSYNmis dynamics that differ by three orders of magnitude, respectively minutes and days.

2.1 Parametric Variation Analysis

The script was adapted in such a way that we could modify each parameter and apply them based on certain conditions (for example, different inputs corresponding to different time frames) while also maintaining a maximum simulation time. To reproduce the plot visible in **Fig. 2b** we maintained standard non-disease conditions for $S_{2,3,4}$ while we set S_1 to 2.6 from days 10 to 150. Moreover, we tried varying all parameters, one at a time, to see which allowed to switch to the "disease state", and turning them on and off to see whether the system would naturally go back to a "non-disease state" or not. All parameters were also increasingly/decreasingly varied in time to find the boundary value causing the switch from a state to another.
Additionally, we performed a sensitivity analysis of the parameters by varying them of $\pm 1\%$ starting from the bounds between disease and non-disease states. This was done to see how much the area under the curves (AUCs) would vary when the switch happens versus when the system remains in the same state.
Lastly, we tried simulating the potential effect of a "drug" or a "treatment" that directly affects the efficiency of the ROS or αSYN reactions by applying it for a specific amount of consecutive days separated by certain time intervals (simulating the periodic "intake" of a drug).

2.2 Bifurcation Analysis

Bifurcation analyses were conducted to identify how key biological factors, including toxins exposure (S_1), anti-oxidative mechanisms (S_2), genetic predisposition (S_3), and protein clearance (S_4), influence the system's dynamics and stability. The function for steady-state ROS computation, called SteadyStateROS (found in the *bifurcation_analysis.m* code in the Supplementary Materials), relies on a first term (k1 * (...)) modeling ROS production minus a second term (k2 * ROS * S_2) representing ROS clearance (Equations). The parameters of the function are the ones described in the simplified model implementation (section 2). This function describing the steady-state behavior of ROS was analyzed for each key parameter (S_1, S_2, S_3, S_4) individually, while keeping the remaining parameters fixed at their default values. This approach allowed us to isolate the effect of each parameter on the system's dynamics and to construct bifurcation diagrams that reveal how steady-state ROS concentrations respond to changes in the selected parameter. The script finds the zeros of the function for each value of the parameter range and plots them, making visible the stable and unstable states.

3. Results & Discussion

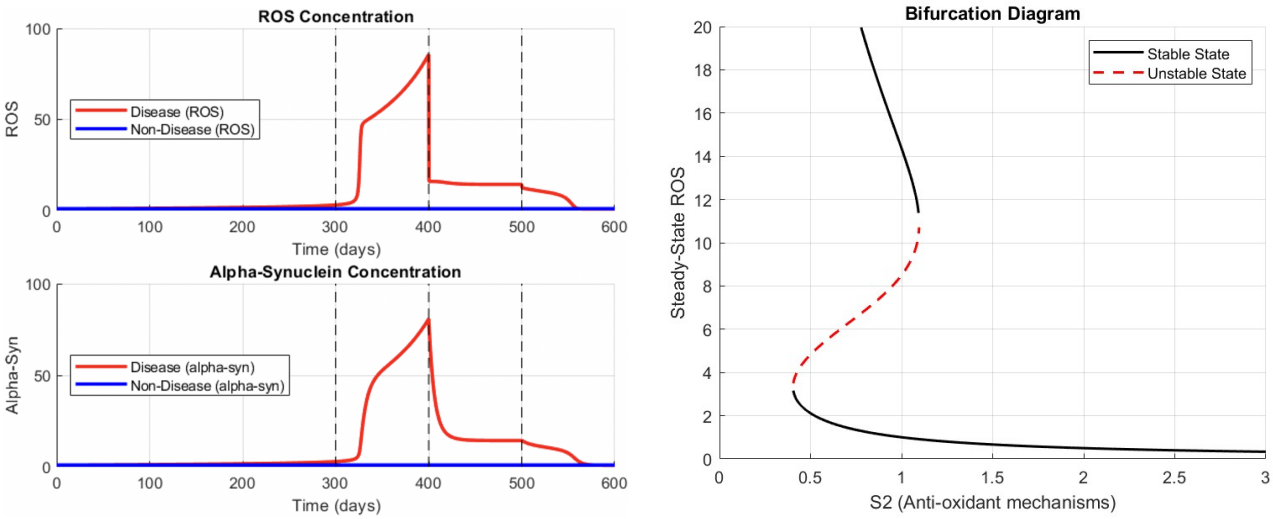

(a) **(b)**

Figure 3. (a) S_2 parameter variation over a period of 600 days. S_2 is decreased progressively for the first 400 days. The dashed line at day 300 represents S_2 reaching the 0.4 boundary value, the one at 400 a switch back to the non disease default value (1) and the one at 500 a higher S_2 of 1.15. **(b)** Relationship between S_2 and the respective steady-state levels of ROS. Black solid lines correspond to stable steady states while red dashed lines to unstable steady states.

The results of the parametric variation analysis and the ones of the bifurcation analysis are in accordance with each other. We report here the analyses results for the S_2 parameter (age-related anti-oxidative mechanisms) (**Fig. 3**).

Figure 3a displays the dynamic variation of ROS and αSYN depending on S_2. The simulation lasts a total of 600 days; for the first 400, the parameter is progressively decreased starting from the default non-disease value of 1. When it reaches 0.4, around day 300, the ROS and αSYN concentrations climb towards the disease state. At day 400 S_2 is reset to 1 and we notice that the system is not able to recover completely to a non-disease state. Finally, at day 500, S_2 is increased furtherly to 1.15, allowing the system to go back to a normal state.

The 0.4 threshold value can also be inferred from the bifurcation plot (**Figure 3b**). Indeed, below this value the system can be found in a disease condition only because of the low anti-oxidative efficiency. The plot shows a bistability region in the 0.4 - 1.1 S_2 range, indicating that perturbations can cause a transition between the two stable states depending on the initial conditions. As S_2 increases, the upper (high ROS) stable branch disappears near 1.1 and the system transitions to the low ROS state, in accordance with the pattern of the previously described plot. This behavior is typical of a 3-equilibria system.

The same concordance between the threshold value found in the parametric variation analysis and the one found in the bifurcation analysis is observed also for the other three parameters S_1, S_3 and S_4. The resulting biological implications are clear: values of toxins exposure (S_1) higher than 2.42 are not compatible with the normal conditions; the same happens for a genetic predisposition value (S_3) higher than 2.48, and for a protein clearance factor (S_4) lower than 0.4. Plots for these three parameters can be found in the Supplementary Materials.

Furthermore, from the sensitivity analysis we can infer that the parameters that have the biggest impact on the system are $S_{1,2,3,4}$

with respect to $k_{1,2,3,4}$, $d_{\alpha\text{SYN}}$ and $K_{\alpha\text{SYN}}$. When varied of 1% from the boundary values, the AUC changed considerably. For example, increasing S_2 from 0.4 to 0.404 dramatically decreases the AUC of almost 90%, corresponding to a passage between disease and non-disease states.

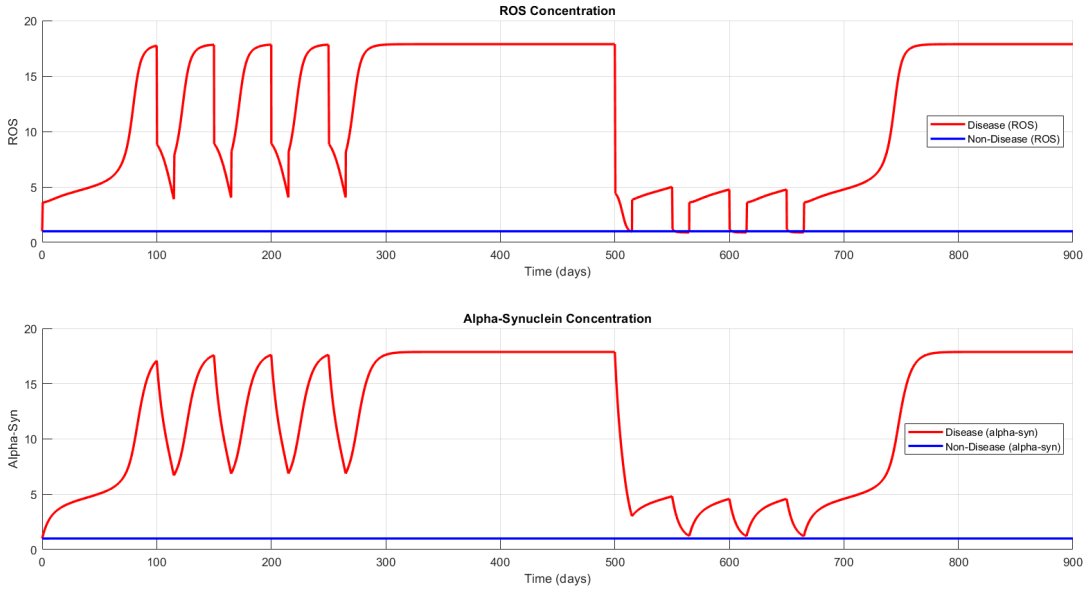

Figure 4. Plot showing the effect of inhibiting the ROS input reaction (*reaction_ROS_1* as found in *PD_simplified.m* in the Supplementary Materials). In a period of 900 days two "drug" intakes are simulated with different efficacies over the same time spans.

Lastly, we tried directly inhibiting the strength of the reactions involving ROS and αSYN, simulating the possible consequence of a drug administration with a continuous stress input ($S_1 = 2.6$). We hypothesized that an effective treatment would target the interaction between misfolded αSYN and ROS production, by impairing the core feedback motif.
Referring to **Figure 4**, we first halved the efficiency of the ROS input reaction for 15 consecutive days with breaks of 35 (periodicity of 50 days). This is visible in the first half of the plot; we can see that the system is not able to maintain a low ROS/αSYN concentration. On the other hand, trying to simulate a "stronger drug", reducing the efficiency of the reaction by 75% over the same period of time, we observe that the curves remain below a concentration of 5μM. This suggests us that a continuous and efficient treatment has the potential to preserve a non-disease condition. Nevertheless, once this type of treatment is not administered anymore (in the figure, at days 300 and 700), the system returns to the disease ROS/αSYN concentrations. The only way to reverse completely the effects of S_1 with a single drug administration is to combine both a decrease in efficiency of the reaction and a reduction of the S_1 parameter itself.

4. Conclusion

To conclude, we assessed that the simplified model simulates well the qualitative behavior of the ROS/αSYN dynamics in PD. Moreover, by exploring the effect of the risk factors, we simulated PD dynamics and observed their concordance with what is reported in literature. This furtherly strengthens the reliability of the implemented model. Additionally, the drug simulation analysis provided valuable insights into potential therapeutic strategies. Targeting the core feedback loop involving ROS and αSYN demonstrated that treatments with sufficient potency and continuity could temporarily preserve a non-disease state. Finally, the study highlights the multifactorial nature of PD, where interactions among these risk parameters play pivotal roles in disease progression.

Acknowledgments

We want to express our appreciation to Professor Andrea Pugliese and to Elena Righetti for their support during the "Mathematical Modeling in Biology" course.

Abbreviations

PD: Parkinson's Disease; **ROS:** Reactive Oxygen Species; **αSYN:** alpha-synuclein; **LB:** Lewy Bodies; **ODE**: Ordinary Differential Equation; **AUC:** Area Under the Curve.

References

[1] Lorraine V Kalia and Anthony E Lang. Parkinson's disease. *The Lancet*, 386(9996):896–912, 2015.

[2] Eduardo Tolosa, Alicia Garrido, Sonja W Scholz, and Werner Poewe. Challenges in the diagnosis of parkinson's disease. *The Lancet Neurology*, 20(5):385–397, 2021.

[3] M. Cloutier and P. Wellstead. Dynamic modelling of protein and oxidative metabolisms simulates the pathogenesis of parkinson's disease. *IET Systems Biology*, 6(3):65–72, 2012.

[4] M. Cloutier, R. Middleton, and P. Wellstead. Feedback motif for the pathogenesis of parkinson's disease. *IET systems biology*, 6(3):86–93, 2012.

[5] Rahuman S Malik-Sheriff, Mihai Glont, Tung V N Nguyen, Krishna Tiwari, Matthew G Roberts, Ashley Xavier, Manh T Vu, Jinghao Men, Matthieu Maire, Sarubini Kananathan, Emma L Fairbanks, Johannes P Meyer, Chinmay Arankalle, Thawfeek M Varusai, Vincent Knight-Schrijver, Lu Li, Corina Dueñas-Roca, Gaurhari Dass, Sarah M Keating, Young M Park, Nicola Buso, Nicolas Rodriguez, Michael Hucka, and Henning Hermjakob. BioModels — 15 years of sharing computational models in life science. *Nucleic Acids Research*, 48(D1):D407–D415, 1 2020. gkz1055.

Supplementary Material

Supplementary material and figures, together with the Matlab codes utilized in our analysis can be found in the GitHub repository at the following link: `https://github.com/Sara-Baldinelli/MM-project`

Variables and Parameters

Symbol	Value	Description
ROS	1μM (steady-state)	Concentration of ROS
αSYNmis	1μM (steady-state)	Concentration of misfolded αSYN
k_1	$720\mu M h^{-1}$	ROS generation rate
k_2	$720h^{-1}$	ROS removal rate
k_3	$0.007h^{-1}$	αSYNmis generation rate
k_4	$0.007h^{-1}$	αSYNmis removal rate
$d_{\alpha\text{SYN}}$	15 (dimentionless)	Increase in ROS release due to αSYN damage
$K_{\alpha\text{SYN}}$	8.5μM	Hill kinetic constant for αSYN damage
S_1	0 (non-disease)	Internal/external oxidative stresses
S_2	1 (non-disease)	Age-related anti-oxidative mechanisms
S_3	1 (non-disease)	Influence of genetic mutation/damage
S_4	1 (non-disease)	Protein clearance mechanisms

Table 1. Table of the modeled variables (ROS and αSYNmis) and parameters, together with their default values and explanation.

Equations

$$v_1 = k_1\left[1 + S_1 + d_{\alpha\text{SYN}}\left(\frac{(\frac{\alpha\text{SYNmis}}{K_{\alpha\text{SYN}}})^4}{1+(\frac{\alpha\text{SYNmis}}{K_{\alpha\text{SYN}}})^4}\right)\right] \qquad v_2 = k_2 \times ROS \times S_2 \qquad \frac{\partial ROS}{\partial t} = v_1 - v_2$$

$$v_3 = k_3 \times ROS \times S_3 \qquad v_4 = k_4 \times \alpha\text{SYNmis} \times S_4 \qquad \frac{\partial \alpha\text{SYNmis}}{\partial t} = v_3 - v_4$$

Bifurcation Analysis

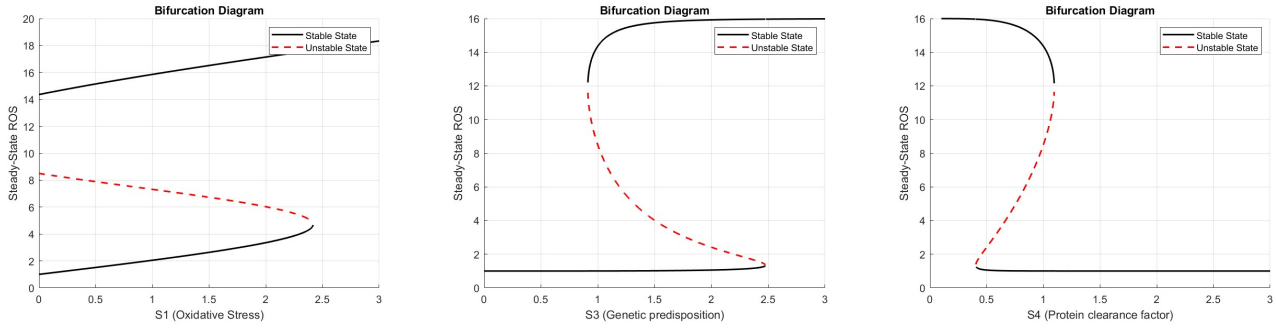

(a) **(b)** **(c)**

Figure 5. Bifurcation diagrams for S_1, S_3 and S_4. Black solid lines correspond to stable steady states while red dashed lines to unstable steady states.